

FIRST TERRASAR-X INTERFEROMETRY EVALUATION

Nico Adam, Michael Eineder, Birgit Schättler and Nestor Yague-Martinez

DLR, Oberpfaffenhofen, 82234 Wessling, Germany, nico.adam@dlr.de

ABSTRACT

The German radar satellite TerraSAR-X was launched in June 2007 [1] and is currently ending its commissioning phase. We anticipate quite different interferometric application scenarios compared to ERS-1/2 and ASAR due to the X-band frequency, the short orbital repeat cycles of 11 days, the high range resolution and the spotlight mode of this sensor.

During the commissioning phase we have scheduled a number of acquisitions over selected test sites with different characteristics to get an early quick look of TerraSAR-X's interferometric capabilities and to assess the phase quality of the sensor and DLR's processor system [2].

Our first results are quite encouraging and the technical parameters of the system are as specified. Many spectacular image details let us expect that the high resolution will demand a different view on SAR interferometry and allow new applications in urban environments.

In our paper we show interferograms and images of different test sites, coherence measurements and a first assessment of the interferometric properties. We will give hints to future scientific users on data selection and data processing.

The results are of high relevance for the TanDEM-X mission scheduled for 2009, when a second compatible SAR-sensor will be launched for a joint 3 year bistatic interferometric formation flight.

1 SENSOR AND INSAR PROCESSING DETAILS

The TerraSAR-X satellite has been launched on 15th of June 2007. It provides high resolution and short wavelength SAR imagery at a repeat cycle of only 11 days [3] allowing new interferometric applications. Most interesting for interferometry are the *strip map*, the *spotlight* and the *high resolution spot light* mode of the sensor. The tables 1-3 list some characteristic parameters of the different acquisition modes in single polarization.

Table 1: Strip map mode data

range bandwidth	150 MHz
scene coverage azimuth	50 km
scene coverage range	30 km
azimuth resolution	3.3 m
slant range resolution	1.2 m

Table 2: Spotlight mode data

range bandwidth	150 MHz
scene coverage azimuth	10 km
scene coverage range	10 km
azimuth resolution	2 m
slant range resolution	1.2 m

Table 3: High Resolution Spotlight mode data

range bandwidth	150 MHz / 300 MHz
scene coverage azimuth	5 km
scene coverage range	10 km / 6 - 10 km
azimuth resolution	1.1 m
slant range resolution	1.2 m / 0.6 m

Different algorithms of the interferometric processing need to be adapted in actual processing chains in order to cope with the high resolution and the spotlight acquisition principle. E.g. the coregistration procedures used with the current sensors are not sufficient any more. Typically, a misregistration in the order of a 10th of a sample can be tolerated otherwise the interferometric coherence is reduced [4]. For the sensors ERS and Envisat ASAR the topography induced pixel shift can be modelled by low order polynomials for the whole scene. Fig. 1 and Fig. 2 visualize the sensitivity of the coregistration regarding topography and the error introduced by a polynomial modelling of the mutual shifts.

The high resolution of the sensor TerraSAR-X results in a severe impact of the topography on the mutual shift of the master and slave samples [5]. Fig. 3 and Fig. 4 visualize that the topography induced mutual pixel shift and that their polynomial modelling results in a misregistration in the order of one sample leading to severe loss of coherence and can therefore not be tolerated any more. DLR's interferometric system GENESIS uses a coregistration based on the observation geometry [6]. The mutual shift is estimated for each pixel utilizing a DEM and the precise orbit information. Fig. 8 provides an example for the performance of the algorithm compared to a conventional coregistration.

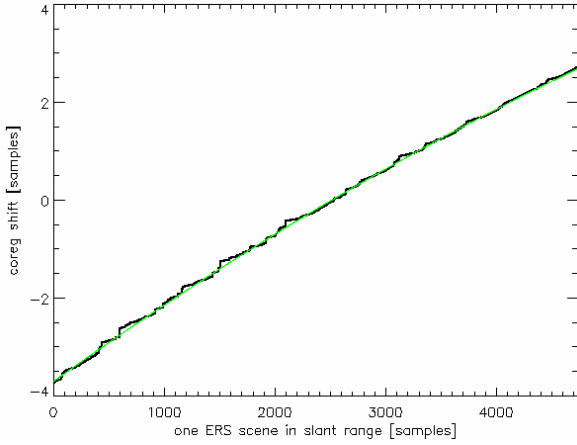


Fig. 1: Topography induced sample shift over range for the sensor ERS; the green line is the optimal polynomial modelling of the shifts

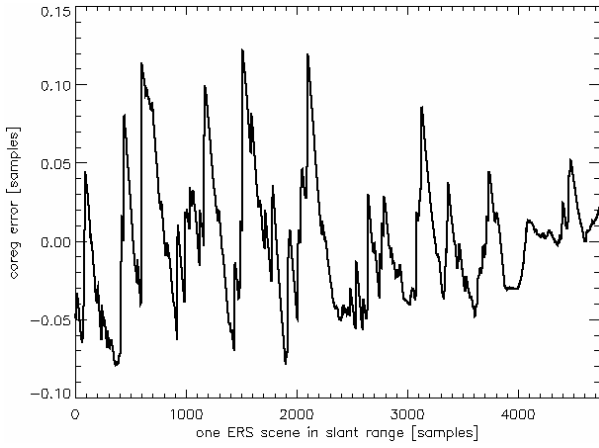


Fig. 2: Error caused by polynomial modelling of the shifts for ERS (difference between black and green line in Fig. 1). The deviation in the order of 10^{th} sample can be tolerated.

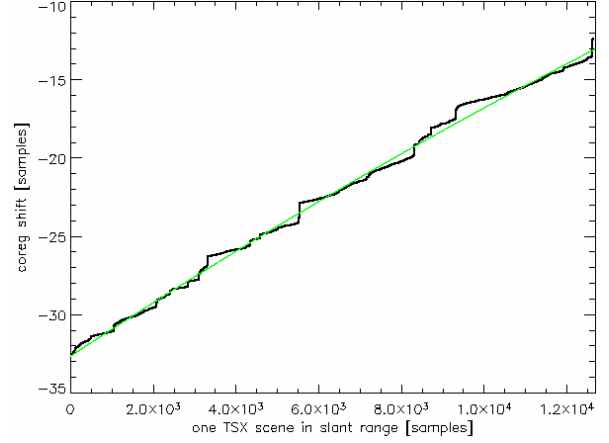


Fig. 3: Topography induced sample shift over range for the sensor TerraSAR-X; the green line is the optimal polynomial modelling of the shifts

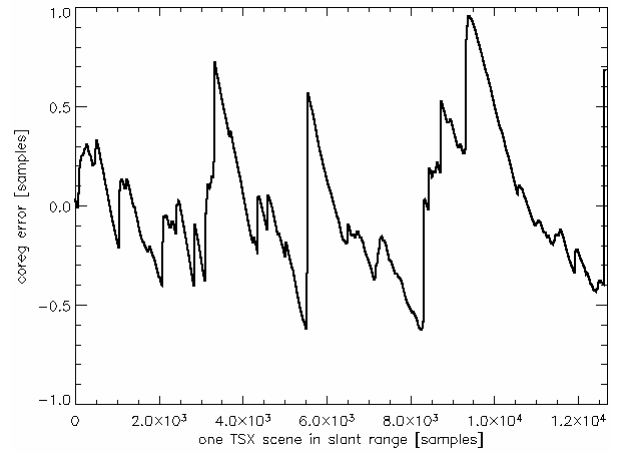


Fig. 4: Error caused by polynomial modelling of the shifts for TerraSAR-X (difference between black and green line in Fig. 3). The deviation in the order of one sample can not be tolerated any more.

The spotlight acquisition is characterized by an azimuth varying Doppler frequency which is caused by the steering of the radar beam. Fig. 5 visualizes a typical Doppler spectrum. Algorithms like the resampling and spectral shift filtering need to be adapted to cope with such spectra. The TerraSAR-X product provides the Doppler frequency polynomials describing the raw data [7]. However, the interferometric processing is based on focussed SSC data and the azimuth time annotation t_{RAW} of the Doppler polynomials needs to be corrected to zero Doppler coordinates using the FM-rate:

$$t_{SSC} = t_{RAW} + \frac{f_{DC}(t_{RAW})}{FM} \quad (1)$$

The object spectra of the two scenes can be misaligned shown in principle in Fig. 6 and need to be spectral shift filtered in order to remove non common spectral components. The DLR GENESIS implementation de-

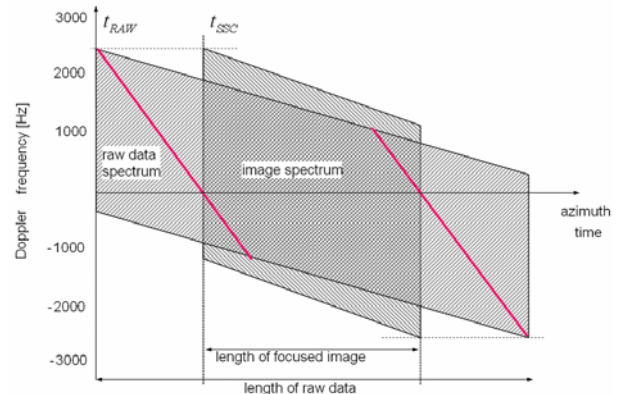


Fig. 5: Typical Doppler spectrum of a spotlight product. Annotated is the raw data timing, however in the InSAR processing the focussed (SSC) timing is used.

ramps the azimuth spectrum using a chirp and then applies a band pass filter in the corrected spectral domain. After filtering the chirp is used to get back the original shape of the Doppler spectrum (up-ramping).

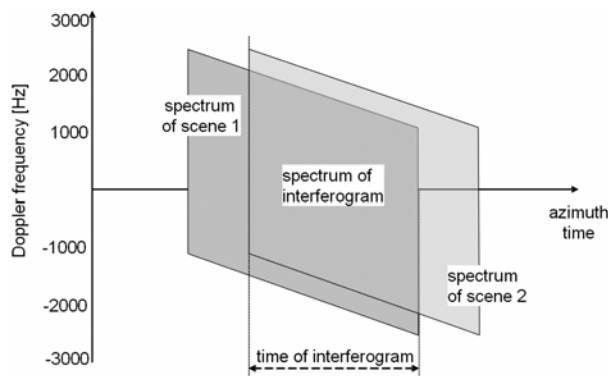


Fig. 6: Principle of the common band filtering in azimuth

2 INTERFEROMETRIC PROPERTIES

The repeat cycle of the sensor is eleven days only. However, a fast temporal decorrelation can be expected in vegetated areas due to the short radar wavelength. Fig. 9 provides a typical TerraSAR-X interferogram. The phase and the coherence image show that forested areas decorrelate but man made structures e.g. roads and buildings remain coherent. Their surface is rough compared to the short wavelength and provides enough return power to be seen by the radar. This is a remarkable property and has immense impact on the TerraSAR-X interferometric applications. The persistent scatterer methodology will change. With the current sensors (e.g. ERS and Envisat ASAR) only point scatterers, called permanent scatterers (PS) [8], could be found to be phase stable over a long observation time span. TerraSAR-X data allow to use both scatterer types i.e. distributed scatterer of man made rough surfaces and the point scatterers. The point scatterers are given by chance. We generally find 100 up to 400 PS per square kilometre in typical urban areas for the current SAR sensors. The high resolution allows to detect and use more PSs. The reason is that the scatterers can better be separated and the signal to clutter ratio (SCR) improves due to the reduced resolution cell's clutter radar return. The better SCR improves the detection of the PS and the precision of the distance related phase measurement. Now many PS per building can be identified and an example is provided in Fig. 7. A typical high resolution spotlight interferogram covering an urban area is shown in Fig. 10.

The time series analysis benefits from the short radar wavelength. A line-of-sight (LOS) deformation maps into phase with about 1.5 cm per phase cycle and is approximately twice as sensitive compared to the

current C-band sensors. Time series analyses for deformation monitoring profit from the three times faster build-up of data stacks which mitigate PU and motion modelling problems.



Fig. 7: St. Luke's Tower in Tokyo; left: photo of the building; right: SCR estimation on the building showing the point scatterers (resolution: 1m x 0.6m)

3 INTERFEROMETRIC EXAMPLES

The capability of TerraSAR-X for interferometric applications is demonstrated by examples on the generation of DEMs, differential interferometry and on a displacement monitoring similar to the PSI technique.

Fig. 11 shows a visualisation of a DEM generated from spotlight acquisitions. The DEM has a spacing of 5 m x 5 m, a coverage of 8 km x 10 km and a vertical accuracy in the order of 5 m. It could be generated 24 hours after the acquisition of the second scene. It provides a preview on the DEMs that will be generated in the Tandem mission [9].

Fig. 12 shows a detail of the Las Vegas test site covering the Convention Center building. The intensity image is radiometrically enhanced by 8 temporal looks. The coherence estimate indicates a high phase stability on the man made features (e.g. the building's roof). Fig. 13 provides interferograms showing the LOS displacement only. They are generated from small baseline interferograms or synthesized removing the topography induced phase.

Fig. 14 provides a deformation monitoring of the Las Vegas spot light data similar to the persistent scatterer method. The Convention Center roof is assumed to be flat with a constant height for the different parts of the building. Each region of the roof is assigned a reference point and a relative estimation regarding this point is performed. I.e. the building's height is compensated and the measured displacement is relative to the regions reference point. No temporal deformation model is

assumed in the assessment applying a simple phase unwrapping (PU) in time - alternatively even a PU in space is possible.

4 SUMMARY

The SAR sensor TerraSAR-X provides high resolution data which allow many new interferometric applications. The generation of DEMs, the displacement monitoring by conventional D-InSAR and the PSI processing are demonstrated with examples. The interferometry profits from the short radar wavelength, the high PS density, the high sensitivity regarding displacements (ca. 1.5 cm/cycle) and the coherent rough surfaces of man made features e.g. roads and buildings. The short repeat cycle of 11 days allows a fast stack build-up and the mitigation of PU problems. However, the high resolution and the spotlight mode require algorithmic adaptations in actual processing chains e.g. the coregistration and the spectral shift filtering. Radargrammetry and InSAR complement each other due to the high resolution.

REFERENCES

- [1] Werninghaus R., Buckreuss S., Pitz W. *TerraSAR-X Mission Status*. Proc. IGARSS 2007, Barcelona, Spain, July 2007
- [2] Breit H., Boerner E., Mittermayer J., Holzner J., Eineder M., *The TerraSAR-X Multi-Mode SAR Processor – Algorithms and Design*. Proc. of 5th EUSAR, Ulm, Germany, 2004
- [3] Schättler B., Fritz T., et al, *TerraSAR-X SAR Payload Data Processing – A Commissioning Phase Perspective*. ASAR 2007, Vancouver, Canada, 2007
- [4] Just D., R. Bamler. *Phase Statistics of Interferograms with Applications to Synthetic Aperture Radar*. Applied Optics, 33(20):4361-4368, July 1994
- [5] Bamler R., Eineder M., *Accuracy of differential shift estimation by correlation and split-bandwidth interferometry for wideband and delta-k SAR systems*. IEEE Geoscience and Remote Sensing Letters, Volume: 2, Issue: 2, pp. 151- 155, April 2005
- [6] Adam, N., B. Kampes, M. Eineder, J. Worawattanamateekul, und M. Kircher. *The development of scientific permanent scatterer system*. Proc. ISPRS 2003, Hannover, Germany, Oct 2003.
- [7] Fritz T., *TerraSAR-X Ground Segment Level 1b Product Format Specification*, TX-GS-DD-3307, Issue: 1.3, Date: 10.12.2007
- [8] Ferretti A., Prati C., Rocca F., *Permanent Scatterers in SAR Interferometry*. IGARSS'99, Hamburg, Germany, 1999
- [9] Fritz T., Breit H., Eineder M., Adam N., Balzer W., *TanDEM-X Interferometric SAR Data Processing Chain*. ASAR 2007, Vancouver, Canada, 2007

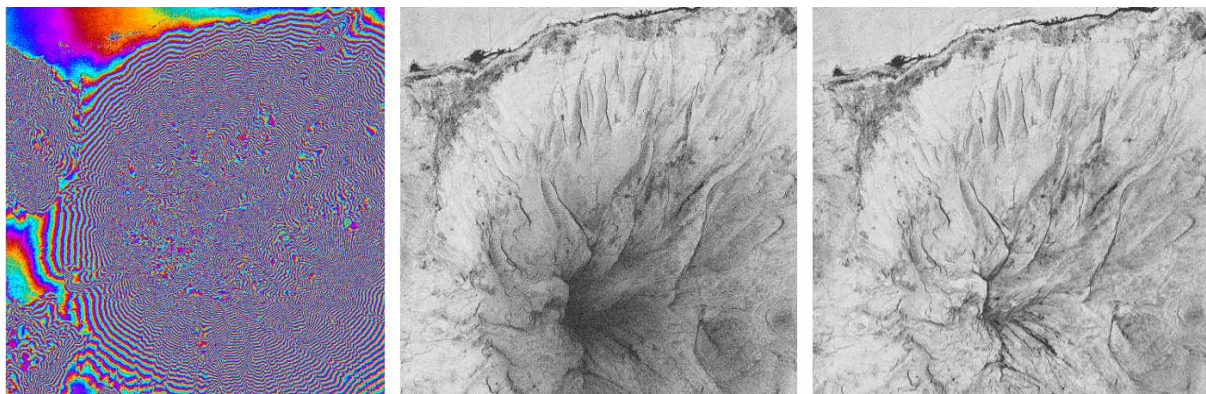


Fig. 8: Example for the DEM supported coregistration. Left: interferogram of a mountain with a height of about 1300 m. Middle and right: Coherence images of the polynomial and topography based coregistration modelling respectively. The 1.3 pixel misregistration is only compensated in the DEM supported algorithm visible on the better coherence.

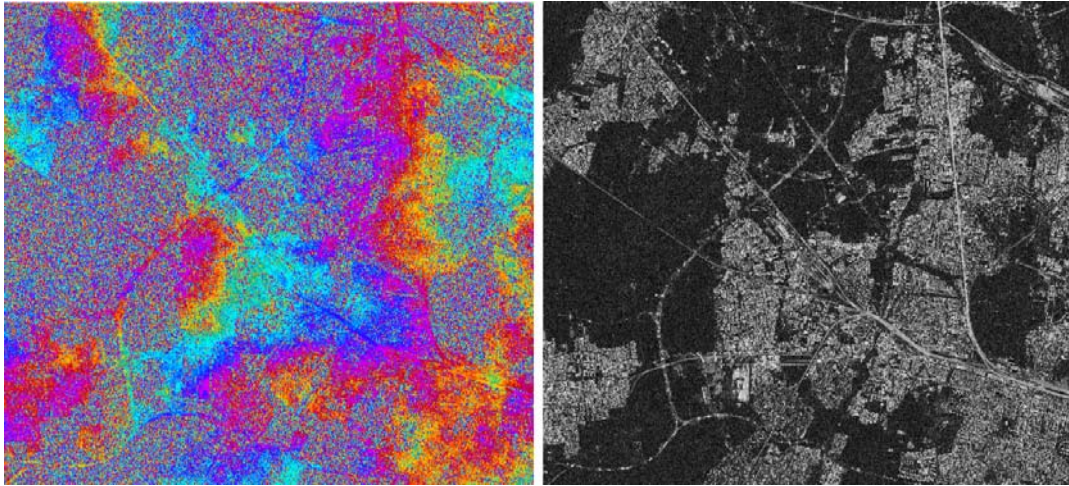


Fig. 9: Interferogram and coherence of the Oberpfaffenhofen test site Strip Map with look angle 46° and height ambiguity of $89 \text{ m}/2\pi$; Forested areas decorrelate but man made structures e.g. roads and buildings remain coherent.

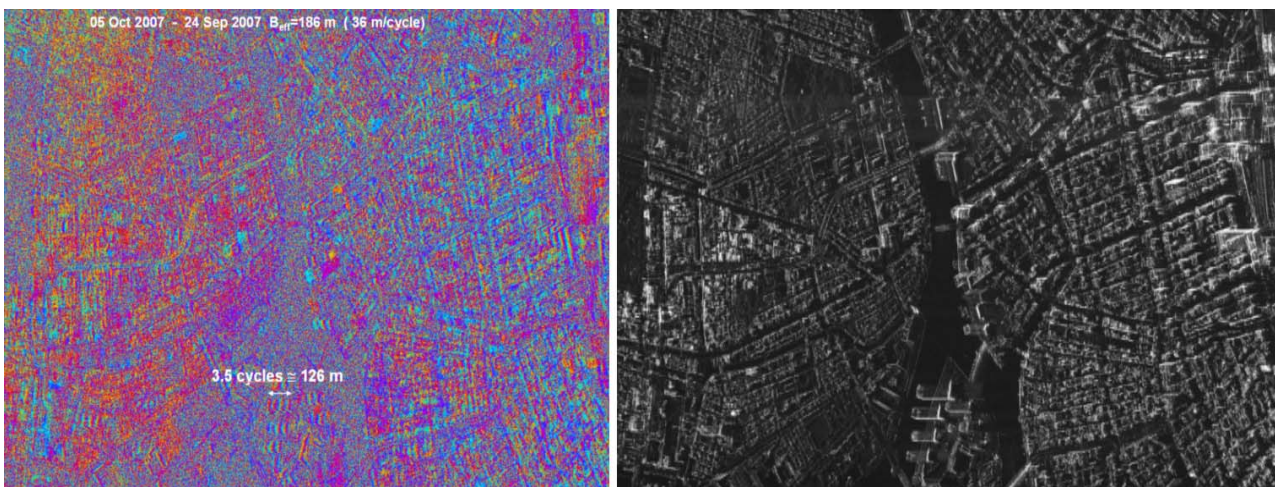


Fig. 10: Left: 300 MHz high resolution spotlight mode interferogram of the city of Tokyo. The baseline is 186 m and consequently one phase cycle represents 36 m height. The height of buildings can be estimated by counting their fringes. right: mean intensity of the test site radiometric enhanced by 5 temporal looks

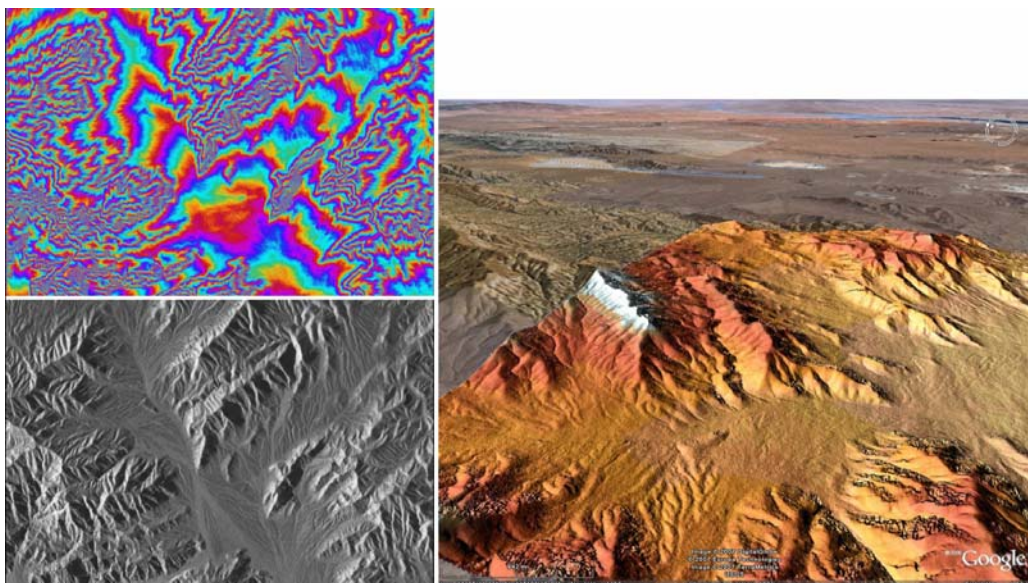


Fig. 11: Visualisation of an interferometric DEM with 5 m spacing and ca. 5 m vertical accuracy generated from spotlight mode data (coverage 8 km x 10 km)



Fig. 12: Crop from the spotlight test site Las Vegas covering the Convention Center building; left: mean intensity radiometric enhanced by 8 temporal looks; right: the coherence estimate indicates a high phase stability on the man made features (e.g. the building's roof)

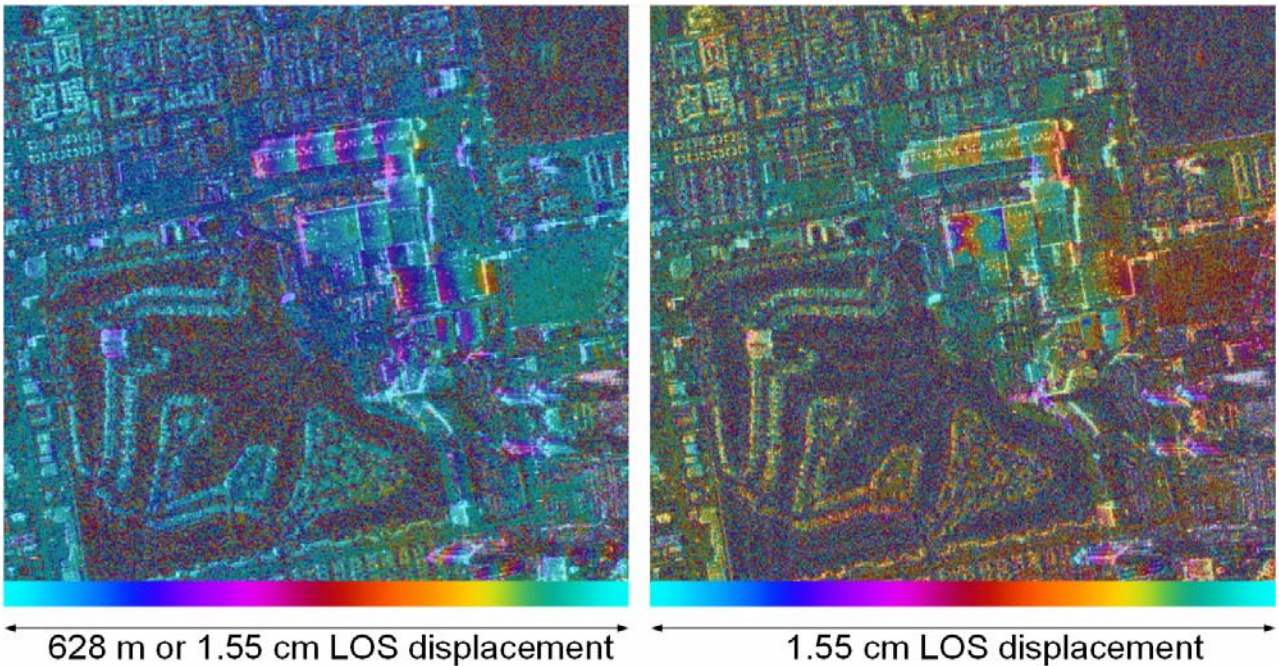


Fig. 13: Examples for a D-InSAR application using TerraSAR-X spotlight data of the Las Vegas test site. The colours indicate a displacement i.e. the structural stress of the building. left: small baseline interferogram which is insensitive to the buildings height showing displacement only; right: synthesized interferogram compensating the topography induced phase showing another displacement period

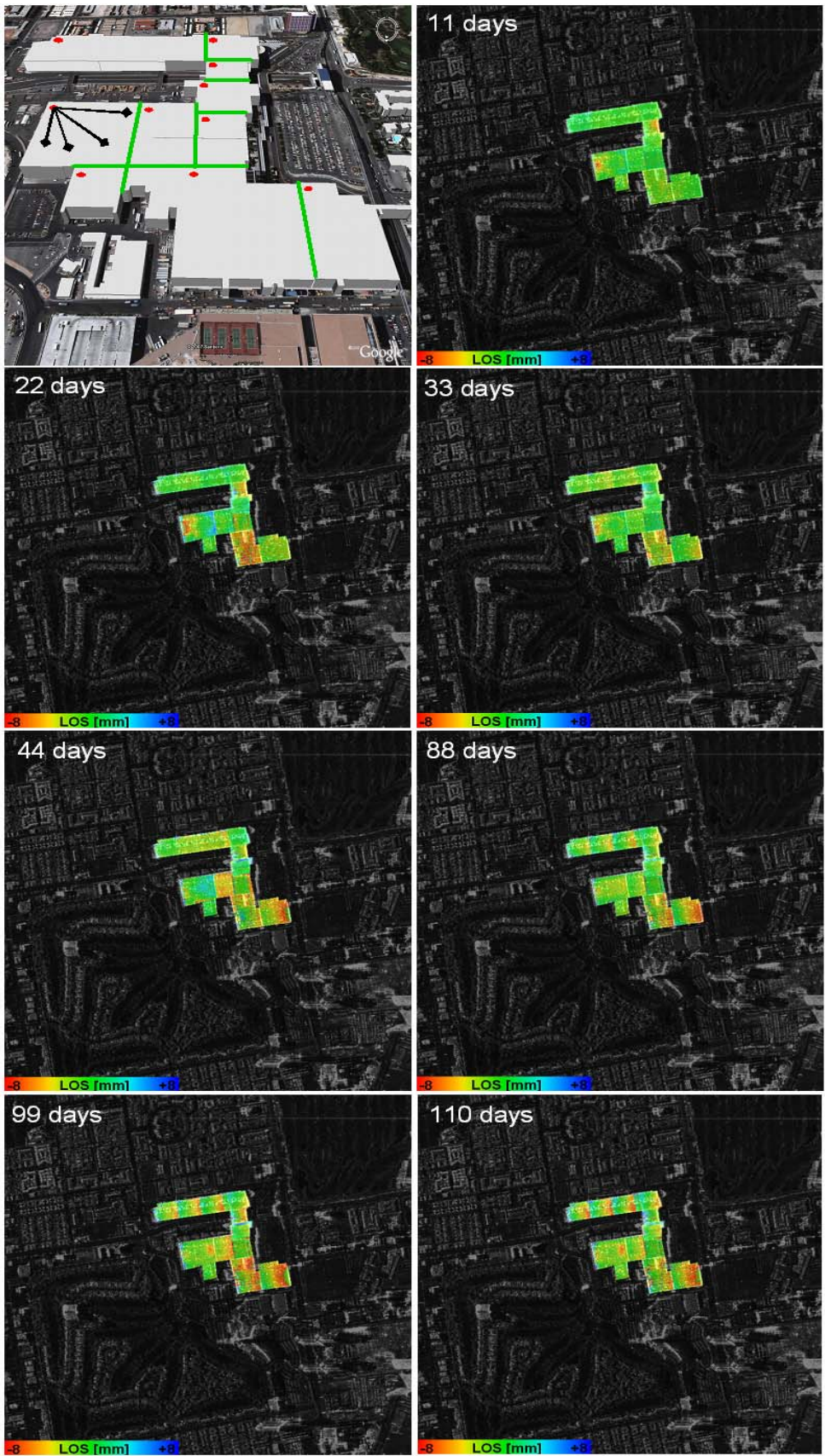


Fig. 14: Displacement monitoring of the Las Vegas Convention Center building similar to the persistent scatterer method, however distributed scatterer are used in the assessment